Chalcogenide Letters Vol. 10, No. 2, February 2013, p. 45 - 53

EFFECT OF ANNEALING TIME AND TEMPERATURE ON STRUCTURAL, OPTICAL AND ELECTRICAL PROPERTIES OF CdS FILMS DEPOSITED BY CBD

J. PANTOJA ENRÍQUEZ[a,b*]
[a]*Centro de Investigación y Desarrollo Tecnológico en Energías Renovables. UNICACH. Libramiento Norte Poniente No 1150, 29039, Tuxtla Gutiérrez, Chiapas, México.*
[b]*Universidad Politécnica de Chiapas. Calle Eduardo J. Selvas S/N. Col. Magisterial, 29010, Tuxtla Gutiérrez, Chiapas, México.*

Cadmium sulphide (CdS) thin films were deposited onto glass substrates by chemical bath deposition (CBD) from a bath containing cadmium acetate, ammonium acetate, thiourea and ammonium hydroxide. The CdS films were annealed in air at various temperatures (350, 400 and 450 °C) for 60 minutes, and times (5, 15, 30, 45 and 60 minutes) at constant temperature (400 °C) in order to investigate the influence of post-deposition annealing treatments on the structural, optical and electrical properties. The various structural parameters such as grain size, lattice constant and strain, were investigated using XRD. The as-deposited films have the mixed (cubic and hexagonal) phase. The grain size increases due to annealing and grain growth is a function of annealing temperature and time duration. The band gap of the films was calculated from the transmittance data. In general the results showed that the structural, optical and electrical properties of CdS depends on the post-deposition annealing duration and temperatures.

(Received December 14, 2012; Accepted February 4, 2013)

Keywords: Chemical bath deposition, Air annealing, X-ray diffraction, Polycrystalline thin films, Cadmium sulphide, optical properties, Semiconducting films.

1. Introduction

Cadmium sulphide is considered as the best-suited buffer layer for CdTe and $CuIn(Ga)Se_2$ solar cells [1–4]. CdS is a direct band gap semiconductor with E_g=2.42 eV, and can be prepared by different techniques such as close spaced sublimation, sputtering, screen printing, vacuum evaporation, spray pyrolysis, spin coating, electrodeposition, chemical bath deposition (CBD), etc. [4–17]. Among these deposition methods CBD is the most cost-effective and simple approach for depositing CdS thin films. The CdS thin films obtained by this method are uniform, adherent, and reproducible [18-19].

Low series resistance, high transmittance and optimum band gap are very important requirements for the buffer material [20]. So the CdS film should be less resistive, thin to allow high transmission and uniform to avoid short circuit effects [20]. However, generally as deposited CdS thin films show high resistivity and optical transmittance, which can be improved. Post-deposition heat treatment is one of fundamental steps to improve the electrical and optical properties of CdS thin films. During the post-deposition heat treatments, fundamental structural changes happen for the film, which influence the optical and electrical properties of the semiconductor film and hence the device. There are studies about the influence of heat treatments in different atmospheres on the physical properties of CdS thin films [16, 21-29].

Despite the fact that CdS has been investigated extensively from the point of view as a hetero-junction partner to the absorber layer in solar cells, and studied to understand the influence

*Corresponding author: jpe2005@gmail.com

of thermal annealing in oxidizing atmospheres, there are many issues remains that still need to be understood. In this paper we discuss the influence of the annealing in air on the structural, optical and electrical properties of chemically deposited CdS thin films.

2. Experimental

The CdS thin films were deposited on glass slides by the CBD technique described in a previous work [4]. The chemical bath contained 0.033M cadmium acetate ($Cd(OOCCH_3)_2.2H_2O$), 1M ammonium acetate ($CH_3CO_2NH_4$), 0.067M thiourea (H_2NCSNH_2) and 28–30% ammonium hydroxide (NH_4OH). The temperature of the bath was maintained constant at 90°C. All the films used in the present study were deposited simultaneously from the same bath. The films were cut into equal portions ($1cm^2$) to perform the heat treatments, and fresh samples were used for each annealing temperatures. The films annealed in air at 350°C, 400°C and 450°C for 60 minutes were used in this investigation. In order to study the effect of annealing duration, 400°C was selected as the temperature and annealed at different time intervals between 5 and 60 minutes. The thickness of the films was measured using an Alpha Step 100 surface profiler. The XRD measurements were performed using a Rigaku X-ray difractometer with CuK_{α} source with λ=1.5418 Å. The various structural parameters such as lattice constant, grain size and strain have been evaluated. The data were collected over a 2θ range of 20–60 degrees, with a grazing angle equal to 1.5°.

The electrical resistivity of the CdS films was measured at room temperature using the two-probe technique. For this purpose, silver paint electrodes of 2 mm length at 2 mm separation were painted on the samples in a coplanar configuration. The dark current were measured using an HP4140B pico-ammeter/DC voltage source with an applied voltage of 100 V. Prior to this measurement, the samples were kept in dark for 1 day to empty all trapping states. The optical transmittance spectra of the films were recorded in a Shimadzu UV-VIS-NIR spectrophotometer.

3. Results and discussion

3.1. Structural properties

The XRD patterns of CdS thin films, both as deposited (virgin) and annealed in air at different temperatures and time durations are shown in Fig. 1. Fig.1a shows the XRD patterns of CdS films annealed at temperatures of 350, 400 and 450°C. Fig.1b is the XRD patterns of films annealed in air at 400°C for 5, 15, 30, 45 and 60 minutes. For comparison XRD patterns of as-deposited film is included in all figures. It can be seen from the diffraction patterns that the peak intensity changes with the annealing temperature and annealing duration indicating structural changes of material. The identification and assignments of the observed diffraction patterns were carried out using the JPDS 41-1049 Hexagonal (H) and JCPDS 10-0454 Cubic (C) reference patterns. For all samples we have observed that an intense peak appears at approximately 26.507°, which corresponds to the CdS hexagonal plane (002), or cubic plane (111). But, the presence of the peaks (100) and (101) at 24.807° and 28.182° indicate that the phase is hexagonal or at least a mixture of hexagonal and cubic. Nevertheless the presence of doublets approximately at 26.5°, 43.9° and 52° indicate that the films contain a mixture of hexagonal (wurtzite) and cubic (zinc-blende) structures.

The relative intensity of the peaks (100) and (101) increase with the annealing time and temperature, however, the intensity of (002) decreases. The above features indicate recrystallization and a phase transformation from mixed phase to stable hexagonal phase. The presence of mixed phases of cubic and hexagonal in CdS films and phase transformation were also observed before [15, 16, 22, 23, 26, 29].

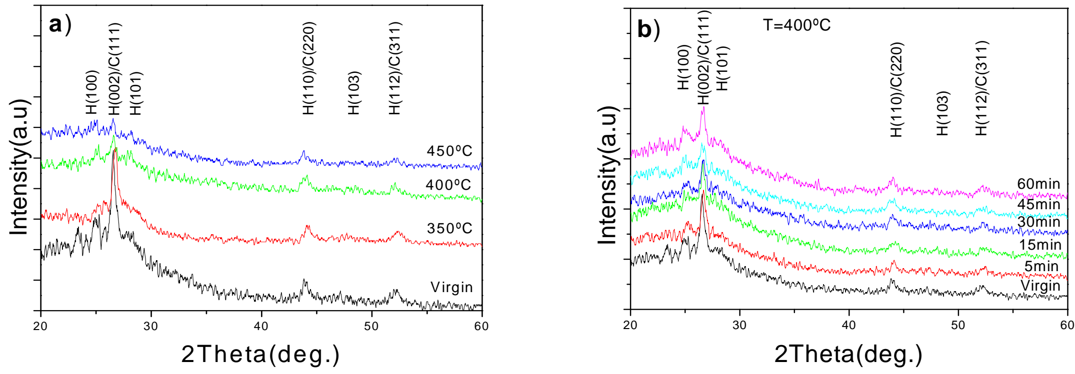

Fig.1. XRD patterns of as-deposited and annealed CdS thin films at different temperature and time duration; a) as-deposited and annealed films at different temperatures, b) XRD patterns of films annealed in air at 400°C for 5, 15, 30, 45 and 60 minutes.

The lattice parameters ***a*** and ***c*** were estimated from the XRD line positions according to the relation [30]:

$$\frac{1}{d_{hkl}^2} = \frac{4}{3}\frac{h^2 + hk + k^2}{a^2} + \frac{l^2}{c^2} \tag{1}$$

where d_{hkl} is the interplanar spacing, and (h,k,l) are the Miller indices. The calculated values of the lattice parameters were later refined using the method developed by Taylor and Nelson [31,32]. In this method the lattice parameters $\mathbf{a}_i$ and $\mathbf{c}_i$ (where i corresponds to a particular XRD line) calculated for different peaks were plotted against $\cos^2\theta(\sin^{-1}\theta+\theta^{-1})$. This graph yields a straight line and the intercept of the graph at $\cos^2\theta(\sin^{-1}\theta+\theta^{-1})=0$ gives the lattice constant of the sample.

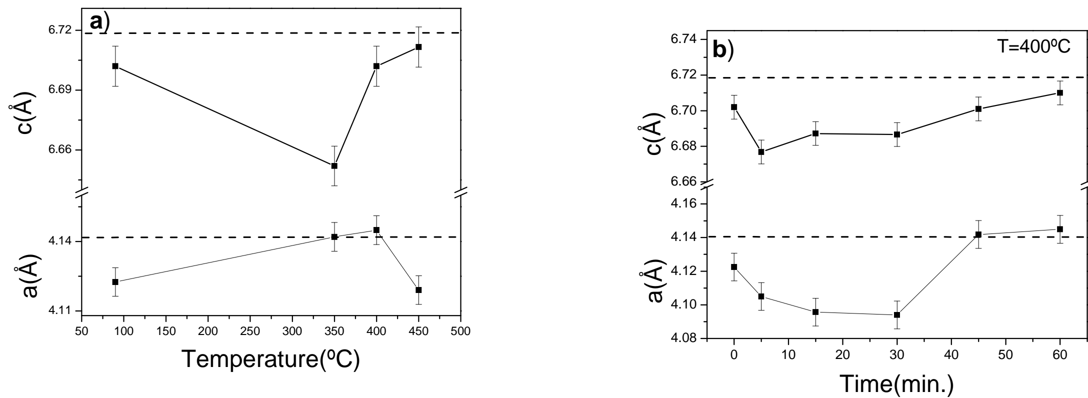

Fig. 2. The variation of lattice parameters a and c as a function of a) annealing temperature and b) annealing time for T=400°C. The dotted straight line corresponds to the stress free value of the lattice constant. The markers are experimental data and the line is a guide to the eye.

The variation of lattice parameters ***a*** and ***c*** as a function of temperature for CdS thin films deposited by CBD is shown in Fig. 2a. It can be seen that the lattice parameters have a dependence on temperature and annealing time. For the as-deposited samples, the value of ***a*** ($\boldsymbol{a}_{\text{as-deposited}}$=4.1225 Å) and ***c*** ($\mathbf{c}_{\text{as-deposited}}$=6.702 Å) are less than the powder sample ($\boldsymbol{a}_{\text{powder}}$=4.1408 Å and $\boldsymbol{c}_{\text{powder}}$=6.7198 Å). The lattice parameter ***a*** of CdS film increase with temperature and reaches a

maximum value for T=400°C and then decrease for T>400°C, while **c**, decreases, and when T>350°C gradually increase as the temperature increases.

Fig. 2b shows the variation of lattice parameters ***a*** and ***c*** of CdS thin films as a function of annealing time for T=400°C. At the initial stages of annealing both ***a*** and ***c*** decrease as the annealing time increases and reaches a minimum in 5 minutes for ***c***, and in 30 minutes for ***a***, then both increase with annealing time. In Fig. 2b, the zero time signifies that of the as-deposited film. These results, indicates that the structural changes are not proportional to the annealing temperature and time.

The average diameter of the CdS grains and the residual strain were calculated from the full-width at half-maximum *(FWHM)* using the relation [33].

$$\beta \cos\theta = K\lambda/D + 4\varepsilon \sin\theta \quad (2)$$

where θ is the Bragg angle and; $\beta^2 = (FWHM)^2 - b^2$, *FWHM* is the full width at half maximum of the peaks, $\lambda=1.54056$ Å is the wavelength of CuK_α radiation, D is the average diameter of the grains, and K is the shape factor which is approximately unity and ε is the residual strain of the films. The integral breadth b, was obtained from a powder sample of polycrystalline silicon. A plot of $\beta\cos\theta$ versus $\sin\theta$ will give a straight line and the grain size D and the strain ε can be calculated from the intercept and slope, respectively.

The variation of the average grain size *D(nm)* with respect to the annealing temperature is presented in Fig. 3a. When the annealing temperature was increased to 450°C, the grain size increases from 18 nm of the as-deposited film to 30 nm approximately. Fig.3b shows the variation of grain size with the annealing time. As one can see from Fig.3b there are three phases for the re-crystallization, in the first phase the grain growth occurs in the first 15 minutes. In this interval the grain size reaches a maximum. The second phase is between 15 and 30 minutes of annealing duration where the grain size decreases. Beyond 30 minutes the grain size remains more or less constant with a tendency to slightly increase in size.

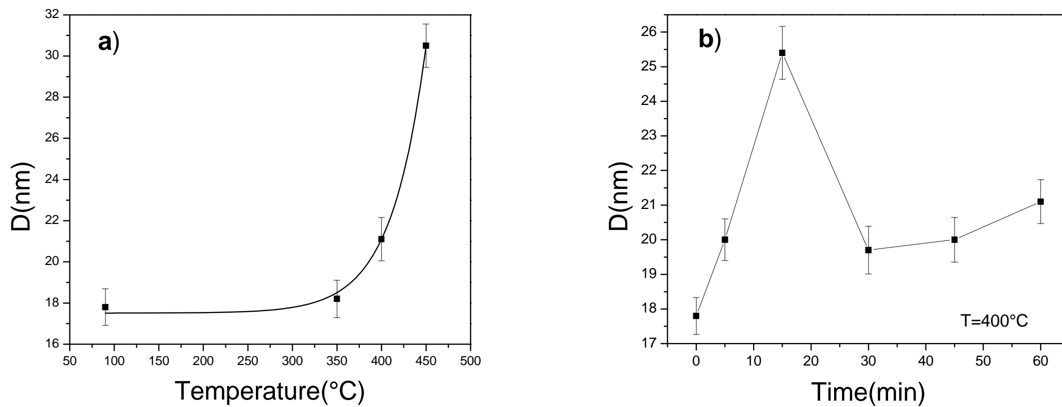

Fig.3. Variation of the average grain size D (Å) with respect a) to the annealing temperature and b) to the annealing duration for annealing temperature of 400°C.

This increase and decrease of the grain size with temperature and annealing duration can be associated in part by two processes that occur during the post-deposition treatment, the process of recrystallization and the loss of material during the annealing. The annealing at lower temperature promotes recrystallization; nevertheless, at high temperatures and long annealing durations the loss of material becomes a very important factor.

Variation of strain in CdS thin films with the annealing temperature is shown in Fig. 4a, and in Fig.4b the dependence of strain on the annealing (T=400°C) duration is demonstrated. The minus sign indicates compressive strain and plus sign indicates tensile strain.

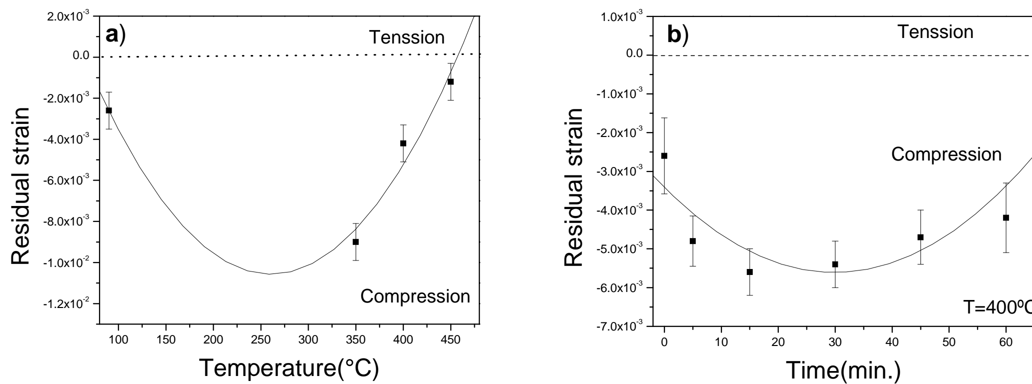

Fig. 4. The dependence of residual strain of CdS films a) on the annealing temperature and b) on the annealing time for T=400°C.

As we can see from Fig. 4a, the as-deposited film is under compressive strain and increases to a maximum value when annealed at 350°C, then decrease with annealing temperature. The dependence of strain on annealing duration when annealed at T=400°C is shown in Fig. 4b. The compressive strain increases with annealing time and reaches a maximum value and then starts to decrease. The change in strain indicates a variation in the concentration of lattice imperfections with the annealing temperature and time.

3.2. Optical properties

Fig. 5 shows the transmittance spectra in the wavelength range of 300–2000 nm for the CdS thin films annealed in air at different temperatures and time duration. Fig. 5a shows the transmittance spectra and the average transmittances in the range of 550–900 nm of CdS films annealed at temperatures of 350, 400 and 450°C. Fig. 5b is the transmittance spectra and the average transmittances in the range of 550–900 nm of films annealed in air at 400°C for 5, 15, 30, 45 and 60 minutes.

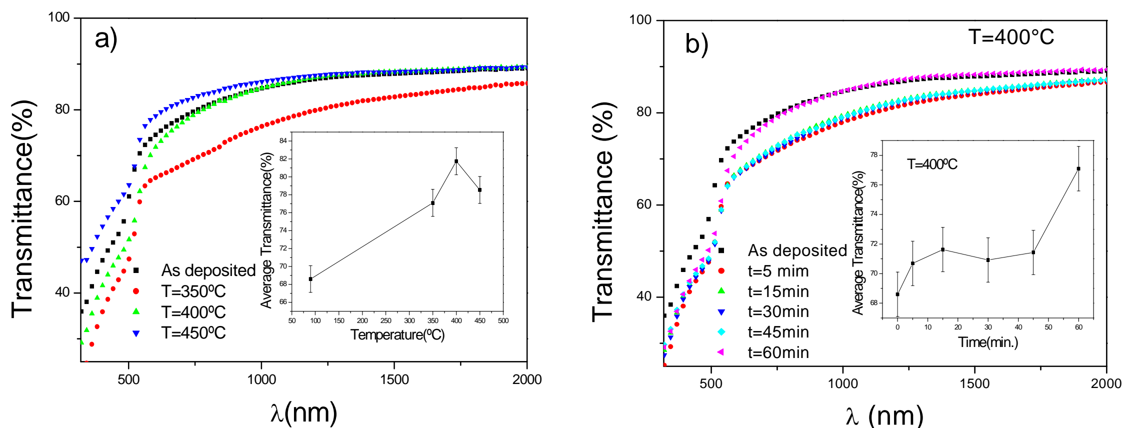

Fig.5. Transmittance spectra of as-deposited and annealed CdS thin films at different temperature and time duration; a) as-deposited and annealed films at different temperatures, b) transmittance spectra of films annealed in air at 400 °C for 5, 15, 30, 45 and 60 minutes. The inset is the average transmittances in the range of 550–900 nm.

From Fig. 5a it can be seen that the average transmittances of CdS thin films increased with the annealing temperature to reach a maximum value of 81.74% at 400 ºC and then decreased to a value of 78.53% at 450 ºC.

The dependence of average transmittance on annealing duration when annealed at T=400°C is shown in Fig. 5b. The average transmittance increases with annealing time. The average transmittance improved compared to the as-deposited CdS thin films because of the decrease in the defect density caused by the annealing process.

The absorption coefficient of the films was calculated from the transmittance spectra near the absorption edge by the relation;

$$\alpha = -\frac{Ln(1/T)}{d} \tag{3}$$

where T is the transmittance and d is the thickness of the film.

In correspondence to the model proposed by Tauc J. [34] and Mott and Davis [35], the absorption coefficient α of the material can be related to the incident photon energy hν through the relation [36-38];

$$\alpha h\nu = A\left(h\nu - E_g\right)^{\frac{1}{2}} \tag{4}$$

where A is a constant, h is the Plank constant, ν is the frequency and E_g is the direct band gap. The band gap of the films was calculated by plotting $(\alpha h\nu)^2$ against $h\nu$. The band-gap values were determined from the intercept of the straight-line portion of *the* $(\alpha h\nu)^2$ against $h\nu$ graph on the $h\nu$ axis.

The dependence of the band gap of CdS films on different temperature and time duration is shown in Fig. 6. The variation of the band gap as a function of temperature for CdS thin films deposited by CBD is shown in Fig. 6a. It can be seen that the band gap decreased from 2.44 to 2.42 eV as the annealing temperature increases from as deposited to 350 ºC and then increased to 2.43 eV above 400 ºC.

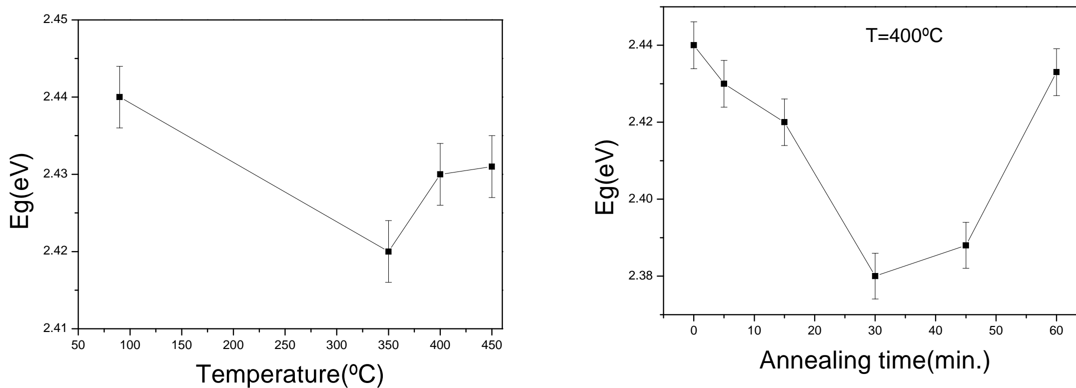

Fig.6. Band gap energy of as-deposited and annealed CdS thin films at different temperature and time duration; a) as-deposited and annealed films at different temperatures, b) band gap energy of films annealed in air at 400°C for 5, 15, 30, 45 and 60 minutes.

Fig. 6b shows the variation of the band gap of CdS thin films as a function of annealing time for T=400°C. At the initial stages of annealing the band gap decrease as the annealing time increases and reaches a minimum in 30 minutes then increases with annealing time.

The parameters and process that affect the band gap are grain size, strain, dislocation density, crystalline phase change from cubic to hexagonal, sulfur and cadmium evaporation that

affect films stoichiometry, oxidation and degradation of the film at annealing temperatures above 400 ºC.

3.3. Electrical properties.

The resistivity of the films under dark was measured and the results are shown in Fig. 7. Fig. 7a shows the resistivity of CdS films annealed at temperatures of 350, 400 and 450°C. Fig. 5b is the resistivity variation of films annealed in air at 400°C for 5, 15, 30, 45 and 60 minutes.

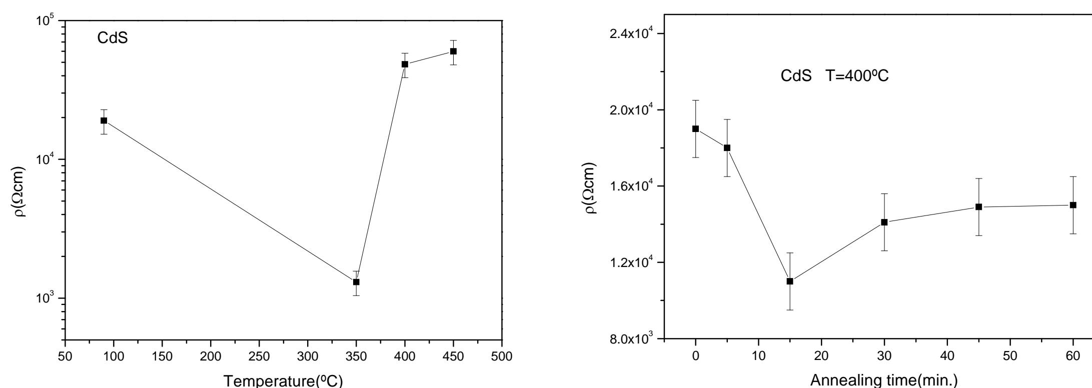

Fig. 7. Dark resistivity of as-deposited and annealed CdS thin films at different temperature and time duration; a) as-deposited and annealed films at different temperatures, b) dark resistivity of films annealed in air at 400 °C for 5, 15, 30, 45 and 60 minutes.

One can see from Fig. 7a that after annealing, the resistivity of the CdS thin films reached a minimum value at 350 ºC and then increased above 350 ºC. Fig. 7b shows the variation of the resistivity of CdS thin films as a function of annealing time for T=400°C. At the initial stages of annealing the resistivity decrease as the annealing time increases and reaches a minimum in 15 minutes then increases with annealing time. Beyond 45 minutes the resistivity remains more or less constant with a tendency to slightly decrease.

The change (decrease and increase) in resistivity, is agreed with the phase transition behavior from the mixed phase to the hexagonal phase (at temperature of 300ºC approximately), increase and decrease (recrystallization and grains disintegration) of grain size, sulfur and cadmium evaporation that affect films stoichiometry and may cause creation of empty spaces in the film, dislocations and imperfections of the films, the oxidation and degradation at high temperature.

4. Conclusions

We have investigated the influence of post-deposition annealing on the structural, optical and electrical properties of CBD prepared CdS thin films. The as-deposited CdS film has a mixture of hexagonal (wurtzite) and cubic (zinc-blende) phases. The recrystallization and phase transformation from mixed phase to stable hexagonal phase occur after the annealing in air. The lattice parameters of as-deposited CdS thin films is lower than that of the powder sample indicating that the as-deposited film is under strain. The grain growth has three stages during the re-crystallization, in the first stage the grains grow in size and attains a maximum, in the second stage the grain size decreases and in the third stage the grain size remains more or less constant with a tendency to increase. The grain growth exponent does not obey the ideal parabolic law. In

general structural, optical and electrical properties of CdS depends on the post-deposition annealing time and temperatures. During annealing the structural, optical and electrical properties are affect for various processes. The first process is the phase transition from the mixed phase to the hexagonal phase (at temperature of 300ºC approximately). The second process is recrystallization and grains disintegration. The third process is sulfur and cadmium evaporation that affect films stoichiometry and may cause creation of empty spaces in the film. The final process may be the oxidation and degradation at high temperature. The annealing at lower temperature promotes recrystallization; however, at higher temperatures or for longer annealing durations the loss of material becomes a very important factor.

Acknowledgements.

The authors acknowledge the technical support of Maria Luisa Ramon Garcia (CIE-UNAM) in XRD measurements. This work was supported partially by the projects SEP-CONACYT CB-2007/83960.

Reference

[1] R.H. Bube, Photovoltaic Materials, (Imperial College Press, London, 1998).
[2] D. Bonnet, Int. J. Solar Energy **12**, 1(1992).
[3] T.L. Chu, S.S. Chu, Solid-State Electron. **38**,533 (1994).
[4] Joel Pantoja Enríquez and Xavier Mathew. Solar Energy Materials & Solar Cells **76**, 313 (2003).
[5] K. Senthil, D. Mangalraj, S. K. Narayandass, Appl. Surf. Sci.**169**, 476 (2001).
[6] P. Taneja, P. Vasa, P. Ayyub, Mater. Lett. **54**, 343 (2002).
[7] M.C. Baykul, A. Balcioglu, Microelectron. Eng. **51,** 703 (2000).
[8] M. Tsuji, T. Aramoto, H. Ohyama, T. Hibino, K. Omura, J. Cryst. Growth **214,** 1142 (2000).
[9] S. Yoshihiko, O. Takashi, J. Vac. Soc. Jpn. **43**, 284 (2000).
[10] A. Luque, S. Hegedus, Handbook of Photovoltaic Science and Engineering, (John Wiley & Sons Ltd., England, 2003)p.617.
[11] A. Rakhshani, A. Al-Azab, J. Phys. Condens. Matter **12**, 8745 (2000).
[12] B. Moon, J. Lee, H. Jung, Thin Solid Films **511–512**, 299 (2006).
[13] J.H. Lee, Thin Solid Films **515**, 6089 (2007).
[14] H. Moualkia, S. Hariech, M.S. Aida, N. Attaf, E.L. Laifa, J. Phys. D: Appl. Phys. **42**, 135404 (2009).
[15] S. Prabahar, M. Dhanam, J. Cryst. Growth **285**, 41 (2005).
[16] H. Metin and R. Esen, *J. Cryst. Growth,* **258**, 141(2003).
[17] S.N. Sharma, R.K. Sharma, K.N. Sood, S. Singh, Mater. Chem. Phys. **93**, 368 (2005).
[18] R.S. Mane, C.D. Lokhande, Mater. Chem. Phys. **65**, 1 (2000).
[19] N. Romeo, A. Bosio, V. Canevari, A. Podesta, Sol. Energy **77**, 795 (2004).
[20] J. Lee, Appl. Surf. Sci. **252**, 1398 (2005).
[21] G. Sasikala, P. Thilakan, C. Subramanian, Sol. Energy Mater. Sol. Cells **62**,275 (2000).
[22] Junfeng Han, Cheng Liao, Tao Jiang, Ganhua Fu, V. Krishnakumar, C. Spanheimer, G. Haindl, Kui Zhao, A. Klein, W. Jaegermann. Materials Research Bulletin **46**, 194 (2011).
[23] Hyeongnam Kim and Donghwan Kim. Solar Energy Materials & Solar Cells **67**, 297 (2001).
[24] K.V. Zinoviev, O. Zelaya-Angel. Materials Chemistry and Physics **70**, 100 (2001).
[25] H. Metin, S. Erat, S. Durmus , M. Ari. Applied Surface Science 256,5076 (2010).
[26] J. Hiie, K. Muska, V. Valdna, V. Mikli, A. Taklaja, A. Gavrilov. Thin Solid Films **516**, 7008 (2008).
[27] Lei Wan, Zhizhong Bai, Zerong Hou, Deliang Wang, Hao Sun, LiminXiong. Thin Solid Films **518**, 6858 (2010).
[28] Dipalee J. Desale, Shaeed Shaikh, FarhaSiddiqui, Arindam Ghosh, Ravikiran Birajdar, Anil Ghule, Ramphal Sharma. Adv. Appl. Sci. Res. **2**, 417(2011).
[29] Wug-Dong Park. Journal of the Korean Physical Society, **54**, 1793 (2009).

[30] B. D. Cullity: Elements of X-ray diffraction (MA, Addison-Wesley Publishing Company, Boston, 1978).
[31] A. Taylor and H. Sinclair, Proc. Phys. Soc. London **57,** 126 (1945).
[32] J. B. Nelson and D. P. Riley, Proc. Phys. Soc. London **57**, 160 (1945).
[33] E. Lifshin, X-ray Characterization of Materials(Wiley-VCH, New York,1999) p. 37.
[34] Tauc J. Amorphous and Liquid Semiconductors, New York Plenum (1974)
[35] Mott N.F, Davis E.A. Electronic Processes in Non-Crystalline Materials Calendron Press Oxford 1979
[36] J.J. Pankove, Optical Processes in Semiconductors, Prentice-Hall, Englewood Cliffs, NJ, 1971.
[37] P. W. Davis and T.S. Shilliday, Phys. Rev. **118**, 1020 (1960).
[38] J.I.Pankove, Optical Processes in Semiconductors, Dover, New York, 1971, p.44.